



HAL
open science

MicroRNA-1291-mediated silencing of IRE1 enhances Glypican-3 expression

Marion Maurel, Nicolas Dejeans, Saïd Taouji, Eric Chevet, Christophe F
Grosset

► **To cite this version:**

Marion Maurel, Nicolas Dejeans, Saïd Taouji, Eric Chevet, Christophe F Grosset. MicroRNA-1291-mediated silencing of IRE1 enhances Glypican-3 expression. *RNA*, 2013, 19 (6), pp.778-788. 10.1261/rna.036483.112 . inserm-02437937

HAL Id: inserm-02437937

<https://inserm.hal.science/inserm-02437937>

Submitted on 14 Jan 2020

HAL is a multi-disciplinary open access archive for the deposit and dissemination of scientific research documents, whether they are published or not. The documents may come from teaching and research institutions in France or abroad, or from public or private research centers.

L'archive ouverte pluridisciplinaire **HAL**, est destinée au dépôt et à la diffusion de documents scientifiques de niveau recherche, publiés ou non, émanant des établissements d'enseignement et de recherche français ou étrangers, des laboratoires publics ou privés.

MicroRNA-1291-mediated silencing of IRE1 α enhances Glypican-3 expression

Marion Maurel^{1,2,*}, Nicolas Dejeans^{1,3}, Saïd Taouji^{1,3}, Eric Chevet^{1,3,4} and Christophe F. Grosset^{1,2,*}

¹Groupe de Recherche sur L'étude du foie, Université Bordeaux Segalen, F-33000 Bordeaux, France. ²Team «Post-transcriptional regulation and Liver Cancer», INSERM, U1053, F-33000 Bordeaux, France. ³Team «Endoplasmic Reticulum stress and cancer», INSERM U1053, F-33000 Bordeaux, France. ⁴CHU de Bordeaux, F-33000 Bordeaux, France.

*Correspondence to : Marion Maurel, m.marionmaurel@gmail.com or Christophe Grosset, christophe.grosset@u-bordeaux2.fr; INSERM U1053, Groupe de Recherche sur L'étude du Foie, Université Bordeaux-Segalen, 146 rue Léo Saignat, Bordeaux, France

Running title: miR-1291-mediated GPC3 upregulation involves IRE1 α

Keywords: microRNA, post-transcriptional up-regulation, GPC3, ERN1, RIDD, FunREG.

ABBREVIATIONS

AMD, AU-rich-mediated decay; ANOVA, one-way analysis of variance; CDS, coding sequence; DF-FunREG, Dual-Fluorescence FunREG system; DTT, dithiothreitol; ER, endoplasmic reticulum; FBS, Fetal Bovine Serum; GAPDH, Glyceraldehyde 3-phosphate dehydrogenase; GFP, Green Fluorescent protein; GPC3, Glypican-3; GPI, glycosylphosphatidylinositol; HCC, hepatocellular carcinoma; miRISC, miRNA-induced silencing complexes; miRNAs, microRNAs; NMD, Nonsense-Mediated mRNA Decay; nt, nucleotide; RIDD, Regulated IRE1 α -Dependent Decay; SD, standard deviation; siRNA, small inhibitory RNA; snoRNA, small nucleolar RNA; Tun, Tunicamycin; UPR, unfolded protein response; UTR, untranslated region.

Accepted version

Abstract

MicroRNAs (miRNA) are generally described as negative regulators of gene expression, however few evidences suggest that they may also play positive roles. As such we reported that miR-1291 leads to *GPC3* mRNA expression increase in hepatoma cells through a 3'-untranslated region (UTR)-dependent mechanism. In the absence of any direct interaction between miR-1291 and *GPC3* mRNA, we hypothesized that miR-1291 could act by silencing a negative regulator of *GPC3* mRNA expression. Based on *in silico* predictions and experimental validation, we demonstrate herein that miR-1291 represses the expression of the mRNA encoding the endoplasmic reticulum (ER)-resident stress sensor *IRE1 α* by interacting with a specific site located in the 5'-UTR. Moreover, we show *in vitro* and in cultured cells that *IRE1 α* cleaves *GPC3* mRNA at a 3'-UTR consensus site independently of ER stress, thereby prompting *GPC3* mRNA degradation. Finally, we show that the expression of a miR-1291-resistant form of *IRE1 α* abrogates the positive effects of miR-1291 on *GPC3* mRNA expression. Collectively, our data demonstrate that miR-1291 is a biologically relevant regulator of *GPC3* expression in hepatoma cells and acts through silencing of the ER stress sensor *IRE1 α* .

Introduction

MicroRNAs (miRNAs) are endogenous ~22nt non-coding RNAs which regulate gene expression by controlling target mRNA translation and/or degradation (Bartel 2009; Fabian et al. 2010; Huntzinger and Izaurralde 2011). In most cases, miRNAs act as post-transcriptional repressors of gene expression through mechanisms involving sequence-specific mRNA:miRNA recognition and the regulated binding of miRNA-induced silencing complexes (miRISC) on target 3'-untranslated region (UTR) (Pillai et al. 2007). In addition, few reports have also demonstrated the existence of miRNA-mediated target induction through molecular processes involving either the direct miRNA:target pairing or an indirect regulation through intermediary factors (Vasudevan 2012). Although the precise mechanisms underlying these phenomena remain elusive, recent evidences have brought some relevant information. For instance, some miRNAs positively regulate gene expression through a direct pairing depending on the cellular context or the site location (e.g. 5'UTR) (Vasudevan et al. 2007; Orom et al. 2008; Vasudevan 2012). This was well illustrated with miR-10a which binds to ribosomal protein RPS16, RPS6 and RPL9 encoding mRNA 5'-UTR and consequently enhances their translation (Orom et al. 2008). MiRNAs have also been implicated in gene up-regulation by targeting promoter elements. This is the case of miR-744 and miR-1186, which induce the transcription of mouse *Cyclin B1* (Huang et al. 2012). Other illustrations of miRNA-dependent gene induction were provided by recent discoveries showing that some miRNAs attenuate Nonsense-Mediated mRNA Decay (NMD) (Bruno et al. 2011) and AU-rich-mediated decay (AMD) (Ma et al. 2010).

In a previous study, we showed that three miRNAs promote Glypican-3 (*GPC3*) expression in hepatoma cells by a mechanism dependent on *GPC3* 3'-UTR (Maurel et al. 2013). *GPC3* belongs to the heparan sulfate proteoglycan family and regulates the signaling pathways mediated by WNTs, Hedgehogs, fibroblast growth factors and bone morphogenetic proteins (Fransson 2003; Filmus et al. 2008). *GPC3* is a glycosylphosphatidylinositol (GPI) membrane-anchored protein that uses the secretory pathway to reach the plasma membrane. *GPC3* is a gene involved in various human diseases including type 1 Simpson-Golabi-Behmel syndrome and Wilms tumors. Moreover *GPC3* is overexpressed in hepatocellular carcinoma (HCC) and hepatoblastoma (Jakubovic and Jothy 2007) in which its expression correlates with tumor aggressiveness and poor prognosis (Shirakawa et al. 2009). To

characterize the miRNAs regulating *GPC3* expression in HCC-derived cells, we screened a library of 876 human mature miRNA mimics using the *GPC3* 3'-UTR as a bait (Maurel *et al.* 2013). MiR-129-1-3p, miR-1291 and miR-1303 promote the up-regulation of *GPC3* mRNA expression through uncharacterized mechanisms all depending on *GPC3* 3'-UTR. Interestingly miR-1291 is more particularly up-regulated in HCC sub-groups that express high levels of *GPC3* (Maurel *et al.* 2013).

In the present study, we investigated the molecular mechanisms by which miR-1291 may induce *GPC3* mRNA expression in hepatoma cells. To this end, an integrated approach combining *in silico* analyses, *in vitro* and cell-based validations was undertaken. We demonstrate that miR-1291 represses the expression of the endoplasmic reticulum (ER)-resident endoribonuclease IRE1 α , which itself promotes *GPC3* mRNA decay. The latter regulation occurs through a mechanism which could be related to the Regulated IRE1 α -Dependent Decay (RIDD) of mRNA (Hollien *et al.* 2009), therefore adding to the repertoire of miRNA-mediated decay mechanisms of repressive protein-associated machineries.

Accepted Version

Results

MiR-1291 targets an intermediate factor that regulates *GPC3* mRNA expression

At first, to characterize the mechanisms involved in miR-1291-mediated *GPC3* mRNA expression increase, we used our previously described FunREG fluorescence reporter system in HCC-derived HuH7 cells (Laloo *et al.* 2009; Maurel *et al.* 2013). The average number of lentiviral transgene copies per cell ('transgene copy number', TCN) was measured by quantitative PCR in HuH7 cells expressing the eGFP-*GPC3* 3'-UTR transgene. Then the cells were transfected with a mature miR-1291 mimic or a control RNA. Three days later, eGFP protein (P) and mRNA (M) expression levels were determined using FACS and RT-qPCR, respectively. Finally P/TCN, M/TCN and P/M ratios, which respectively correspond to the global post-transcriptional regulation, the mRNA stability and the translation efficiency, were calculated (Laloo *et al.* 2009; Laloo *et al.* 2010). As previously reported (Maurel *et al.* 2013), FunREG ratios (Fig. 1) indicated that miR-1291 enhanced eGFP-*GPC3* 3'-UTR expression by ~50%. This effect exclusively resulted from an increased mRNA stability, as the translation efficiency remained unchanged (Fig. 1). Because miR-1291 had no effect on expression of an eGFP transgene bearing a control 3'-UTR in HuH7 cells (Maurel *et al.* 2013), we concluded that miR-1291 stabilizes *GPC3* mRNA through a mechanism involving the 3'-UTR.

In the absence of any direct interaction between miR-1291 and *GPC3* mRNA, we hypothesized that miR-1291 could act on *GPC3* expression by silencing a negative regulator. Bioinformatic analysis of the 83 miR-1291-targets, predicted using miRWalk (Dweep *et al.* 2011) and annotated as post-transcriptional regulators using Gene Ontology (Fig. S1), revealed only 7 candidate genes whose expression products were membrane-bound and only one of them which presented an endoribonuclease activity. A functional clustering analysis of those 7 candidates that integrated the Gene Ontology Biological Process (Fig. S1A), specific molecular properties, including the presence of a trans-membrane domain or specific RNase activity (Fig. S1B) and the Gene Ontology Cellular Compartment (Fig. S1C) which all were parsed through a scoring analysis (Troyanskaya *et al.* 2003) revealed that *ERN1* branched out from the other candidates and presented the highest overall scores (Fig. 2A). *ERN1* displayed an endogenous RNase activity and represented the best candidate that could directly regulate *GPC3* mRNA stability. *ERN1*, also known as inositol-requiring enzyme 1 alpha (*IRE1 α*) is an Endoplasmic Reticulum

(ER)-resident transmembrane protein and a site-specific endoribonuclease activated upon accumulation of misfolded protein in this cellular compartment (ER stress). It is a major sensor of the Unfolded Protein Response (UPR), an adaptive mechanism activated upon ER stress (Calfon et al. 2002; Schroder and Kaufman 2005). The cytoplasmic endoribonuclease domain of IRE1 α was first described to cleave *XBP1* mRNA in metazoans, yielding to its splicing and the production of an active transcription factor in response to ER stress (Walter and Ron 2011). In addition, Hollien and colleagues showed that, upon ER stress, IRE1 α also induces the decay of mRNAs encoding membrane and secreted proteins in fly and mammalian cells through the RIDD pathway (Hollien and Weissman 2006; Hollien et al. 2009; Gaddam et al. 2013). GPC3 corresponds to the latter criteria as this GPI-membrane-anchored protein uses the secretory pathway to reach its final destination, i.e. the plasma membrane. Interestingly, three sites homologous to the 5'-CUGCAG-3' IRE1 α consensus cleavage site previously defined by Oikawa and colleagues (Oikawa et al. 2010) are present in *GPC3* mRNA, including one in the 3'-UTR (Fig. 2B). Moreover, overexpression of IRE1 α in HuH7 cells significantly decreased eGFP-*GPC3* 3'-UTR-mRNA stability (Fig. 2C) and this recombinant mRNA was found associated to the ER cytosolic surface (Fig. S2), as previously observed for other cytosolic protein-encoding mRNAs (Lerner et al. 2003; Pyhtila et al. 2008). These observations led us to hypothesize that miR-1291 might target IRE1 α expression, thereby attenuating its IRE1 α endoribonuclease activity towards *GPC3* mRNA.

Based on the above data, we tested the impact of miR-1291 on *IRE1 α* and *GPC3* mRNA expression in HuH7 cells. Overexpression of miR-1291 led to down-regulation of *IRE1 α* mRNA expression by ~40% (Fig. 2D). The amplitude of this effect was consistent with that observed for most other functional miRNAs (Avraham and Yarden 2012) and was accompanied by the simultaneous increase in *GPC3* mRNA (Fig. 2D). Transfection of HuH7 cells with increasing amounts of a miR-1291 inhibitor (AM1291) led to an increase in endogenous *IRE1 α* mRNA expression and to a decrease of endogenous *GPC3* mRNA expression at concentrations above 90nM (Fig. 2E). At lower concentrations (i.e. 12 to 30nM; Fig. 2E and Fig. S3A), AM1291 efficiently depleted miR-1291 in HuH7 cells (Fig. S3A). However, because the expression of miR-1291 in HuH7 cells is about 500 times higher than that of its *IRE1 α* mRNA target (Fig. S3B), these concentrations were most likely too low to

impact the regulatory effects of miR-1291 on the expression of *IRE1 α* and *GPC3* mRNAs. Collectively these results indicate that miR-1291 regulates *IRE1 α* expression and support the first part of our hypothesis.

***IRE1 α* is a direct target of miR-1291**

MiRWalk (Dweep et al. 2011) predicted that *IRE1 α* mRNA contains a site pairing with miR-1291 in its 5'-UTR. A miRNA:mRNA interaction that was further supported using RNAhybrid ((Rehmsmeier et al. 2004); Fig. 3A). Using eGFP-expressing HuH7 cells bearing the *IRE1 α* 5'-UTR (Fig. 3B), we found that miR-1291 decreased eGFP expression by ~50% whereas AM1291 induced it (Fig. 3C). Moreover deletion of the sequence complementary to the miR-1291 seed within the *IRE1 α* 5'-UTR abolished the observed miR-1291-mediated regulation (Fig. 3C). Using FunREG, we further demonstrated that miR-1291 post-transcriptionally controlled *IRE1 α* expression by destabilizing its mRNA with no effect on translation (Fig. 3D). These data confirmed that miR-1291 regulates *IRE1 α* expression by targeting its 5'-UTR and induces *IRE1 α* mRNA degradation through a classical miRNA-seed recognition process.

Our initial hypothesis raised the possibility that miR-1291 positively controls *GPC3* by repressing the expression of a negative regulator of *GPC3* mRNA stability. Our results pointed toward *IRE1 α* as being this protein. In this context, it would be predicted that the expression of a miR-1291-resistant form of *IRE1 α* mRNA (i.e. devoid of its 5'UTR) would prevent miR-1291-mediated *GPC3* mRNA up-regulation. As anticipated, overexpression of an *IRE1 α* transgene lacking its 5'-UTR in HuH7 cells (Fig. S4A) inhibited miR-1291-mediated up-regulation of *GPC3* mRNA expression and led to a decrease in *GPC3* mRNA expression, thereby confirming the functional relationship between those three genes (Fig. 3E).

***IRE1 α* regulates *GPC3* mRNA expression and stability**

To further investigate the relationship between *IRE1 α* and *GPC3*, *IRE1 α* expression was silenced in HuH7 cells and the cells were then exposed or not to ER stress. Both Dithiothreitol (DTT), which reduces disulfide bonds, and Tunicamycin (Tun), a N-linked glycosylation inhibitor, were used to induce ER stress and to activate *IRE1 α* (Schroder and Kaufman 2005). Both drugs induced *XBP1* mRNA

splicing and these effects were attenuated in *IRE1 α* -silenced cells, thus confirming the activation of the *IRE1 α /XBP1* signaling axis upon ER stress in our experimental system (Fig. 4A). Under the same experimental conditions, miR-1291 expression remained stable (Fig. S5). Interestingly, *GPC3* expression increased at both mRNA (Fig. 4B) and protein (Fig. 4C) levels upon attenuation of *IRE1 α* expression and this occurred independently of ER stress. HuH7 cells were then transfected with miR-1291 to evaluate the effects of miR-1291 towards the *IRE1 α* arm of the UPR. At first, the impact of miR-1291 was evaluated on the expression of *HERPUD*, *GRP94* and *CHOP* mRNAs, gene whose transcription is respectively increased downstream of the ATF6 and PERK arms of the UPR upon ER stress (Schroder and Kaufman 2005). In parallel we monitored *IRE1 α* -mediated *XBP1* mRNA splicing and the RIDD activity under the same conditions. As shown in Figure 5, miR-1291 had no influence on the signaling of ATF6 (Fig. 5A) and PERK (Fig. 5B) arms of the UPR. Indeed *HERPUD*, *GRP94* and *CHOP* mRNA expression was not affected by a variation of miR-1291 expression under basal or ER stress conditions. In contrast, miR-1291 specifically affected *IRE1 α* endoribonuclease activity as shown by the attenuation of *XBP1* mRNA splicing upon ER stress and by the inhibition of the RIDD activity as assessed with the expression of the well-characterized RIDD substrates *PDGFRB*, *COL6A1* and *SCARA3* mRNAs (Fig. 5C). Using actinomycin D to inhibit transcription, we further demonstrated that *IRE1 α* silencing led to *GPC3* mRNA stabilization (Fig. 6A). To test whether *GPC3* mRNA is a genuine stress-independent target of *IRE1 α* , we measured the amount of *GPC3* mRNA in control or stressed cells in the presence or absence of actinomycin D. *GPC3* mRNA expression was similar in control and stressed cells in the presence of actinomycin D thereby suggesting an absence of transcriptional compensatory mechanism that could increase *GPC3* mRNA levels upon ER stress (Fig. 6B). Therefore in our conditions, *GPC3* mRNA appears not to be a target of stress activated *IRE1 α* . Interestingly, the analysis of *SCARA3* mRNA revealed that although the cleavage of this RIDD substrate was enhanced upon ER stress, it was also observed under basal conditions (Fig. 5C). The other RIDD substrates tested, *PDGFRB* and *COL6A1* mRNAs were selectively cleaved upon ER stress (Fig. 5C). These data demonstrate that *IRE1 α* controls *GPC3* mRNA stability independently of ER stress and that miR-1291 selectively targets the *IRE1 α* arm of the UPR.

IRE1 α cleaves *GPC3* through a canonical site located in its 3'-UTR

As mentioned above, *GPC3* mRNA sequence contains 3 sites homologous to the 5'-CUGCAG-3' IRE1 α consensus cleavage site and similar to those found in *XBP1* mRNA (Oikawa et al. 2010). In addition, these 3 sites form P-loop structures, thereby yielding potential cleavage sites for IRE1 α ((Oikawa et al. 2010); Fig. 7A). To test whether IRE1 α cleaves *GPC3* mRNA and to identify these sites, total RNA from HuH7 cells was subjected to an *in vitro* IRE1 α -mediated cleavage assay (Bouchecareilh et al. 2010). RT-PCR was then carried out using primers flanking the 3 predicted consensus sites. Interestingly, only one site among the three predicted appeared sensitive to IRE1 α endoribonuclease activity *in vitro* (Fig. 7B). Indeed, the amount of RT-PCR product corresponding to the site located at nucleotides 2039/40 in *GPC3* mRNA 3'-UTR decreased by ~60% whereas the amount of the four other *GPC3* fragments, as well as the control *GAPDH* mRNA, did not change. This suggests that *GPC3* mRNA contains only one functional *in vitro* IRE1 α -mediated cleavage site located in its 3'-UTR. To further demonstrate the relevance of this cleavage site, *in vitro* transcribed *GPC3* mRNA and its mutant counterpart deleted for the 2039/40 site were subjected to IRE1 α -mediated cleavage. In a model where IRE1 α would cleave *GPC3* mRNA at the 2039/40 site (Fig. 7C), two RNA cleavage products of 1700nt and 300nt, respectively, would be produced. As anticipated, cleavage of wild type *GPC3* mRNA generated two RNA fragments of the expected size (Fig. 7D, left). In contrast, deletion of the 2039/40 site in *GPC3* mRNA abrogated IRE1 α -mediated cleavage (Fig. 7D, right). These results demonstrated that, *in vitro*, IRE1 α cleaves *GPC3* in its 3'-UTR at position 2039/40.

To test the physiological relevance of this observation, we evaluated the capacity of IRE1 α to cleave *GPC3* mRNA in cultured cells. Using targeted RT-qPCR (Iqbal et al. 2008), the amount of each *GPC3* mRNA fragment was measured in HuH7 cells upon siRNA-mediated silencing of 5'-3' exonucleases *XRN1/2* or RNA helicase *SKI2*, the latter mediating the 3'-5' degradation of mRNA through the cytoplasmic exosome (Fig. 8A). Compared to the control and as expected, *SKI2* silencing led to the accumulation of the *GPC3* mRNA fragment upstream of IRE1 α cleavage (Fragment 1) with no effect on the amount of the downstream fragment (Fragment 2; Fig. 8B). In contrast, the silencing of *XRN1* or *XRN2* led to an increase

in Fragment 2 with no effect on the amount of Fragment 1 (Fig. 8B). Therefore the *in vitro* cleavage site present in *GPC3* mRNA also exists in cells. This result was further reinforced as *IRE1 α* silencing led to an increase of all fragments in all conditions, due to the absence of *GPC3* mRNA cleavage (Fig. 8B). To further assess whether miR-1291 up-regulates *GPC3* mRNA through the repression of *IRE1 α* expression and the subsequent decrease in RNase activity, HuH7 cells were transfected with miR-1291 in the presence or absence of siSKI2. *IRE1 α* mRNA, *GPC3* mRNA Fragment 1 and the amplicon framing *IRE1 α* cleavage site were then quantified (Fig. 8C-D and Fig. S4B). As expected, miR-1291 down-regulated *IRE1 α* mRNA expression (Fig. S4B) and subsequently up-regulated *GPC3* mRNA (Fig.8C-D). *SKI2* silencing further increased the amount of Fragment 1 (Fig. 8C), but had no impact on *IRE1 α* mRNA expression (Fig. S4B). Quantification of the amplicon framing the cleavage site revealed that cleavage was reduced upon transfection with miR-1291 both in the presence or absence of *SKI2* and that *SKI2* silencing alone did not impact on *GPC3* mRNA cleavage (Fig. 8D). Hence, our results demonstrated that miR-1291 targets *IRE1 α* through its 5'UTR, thereby attenuating *IRE1 α* -mediated decay of *GPC3* mRNA and consequently leading to increased *GPC3* expression in hepatoma cells.

Accepted Article

Discussion

In this work we characterized the molecular mechanism by which miR-1291 post-transcriptionally controls *GPC3* mRNA expression increase (Fig. 9). Using an integrated approach combining both *in silico* analyses and *in vitro*/cell-based validation, we report that miR-1291 binds to the *IRE1 α* 5'-UTR thus destabilizing its mRNA and leading to its degradation. We also demonstrate the presence of a functional *IRE1 α* cleavage site in *GPC3* mRNA 3'-UTR, thereby indicating that *GPC3* mRNA is a genuine RIDD substrate. Collectively, our data show that miR-1291 up-regulates *GPC3* mRNA expression by down-regulating *IRE1 α* mRNA expression. Therefore our results point toward a novel miRNA-dependent gene expression control mechanism through *IRE1 α* silencing and RIDD attenuation.

MiRNAs generally act as negative regulators of gene expression (Bartel 2009). However, some were also shown to act positively (Vasudevan 2012). Using a functional miRNA screening, we recently identified three miRNAs enhancing *GPC3* expression through a 3'-UTR-dependent mechanism among which miR-1291 (Maurel *et al.* 2013). Little is known about the functional properties of miR-1291 in cells. MiRNAs loci are located in different regions of the genome. Half is intragenic and is encoded by protein-coding genes or non-coding RNA genes. This is the case of miR-1291, which is localized in the *SNORA34* gene (Scott *et al.* 2009; Brameier *et al.* 2011). MiR-1291 expression is down-regulated in renal cell carcinoma (Hidaka *et al.* 2012) and in the peripheral blood of acute myocardial infarction patients (Meder *et al.* 2011). However no functional or pathophysiological roles have been associated with these observations. As there is no predicted miR-1291 binding site on *GPC3* mRNA, we hypothesized that miR-1291 could enhance *GPC3* expression by an indirect mechanism involving an intermediate regulatory factor recognizing *GPC3* mRNA 3'-UTR. Such a mechanism has for instance been illustrated with the targeting of genes involved in NMD (Bruno *et al.* 2011) or in the CCR4-NOT complex (Behm-Ansmant *et al.* 2006).

As one miRNA can target hundreds of different mRNAs, it is likely that many negative regulatory intermediates might be the target of miR-1291 to control *GPC3* expression. To restrict the number of candidates obtained *in silico* to an experimentally testable set, we focused on regulatory factors involved in RNA catabolism and likely acting on a sequence-specific site recognition basis. *In silico*

data pointed towards *IRE1 α* as a potential candidate as this gene fulfilled the above-mentioned criteria (Fig. 2A and Fig. S1). The experimental validation revealed that *IRE1 α* was a direct target of miR-1291 (Fig. 3). Remarkably, miR-1291 specifically paired with a site located in *IRE1 α* 5'-UTR (Fig. 3). MiRNA:5'-UTR target interactions are currently poorly described, likely due to the fact that most of the current bioinformatics tools generate predictions on 3'-UTR sequence and not on the full mRNA sequence, which therefore may introduce a prediction bias. In contrast to most available tools, miRWalk produces information on miRNA-targets interactions gathered on the complete mRNA sequence as well as on the gene promoter (Dweep et al. 2011). Finally, the identification of human miR-1291 orthologues in other mammalian species using miRBase (Griffiths-Jones et al. 2008; Kozomara and Griffiths-Jones 2011) together with the conservation of their binding sites in *IRE1 α* 5'-UTRs and the conserved *IRE1 α* target site in the 3'UTR of *GPC3* mRNA in several species suggest the existence of a general regulatory mechanism in mammals (Fig. S6).

In the past two years, several studies have identified miRNAs whose expression is regulated upon ER stress. Each one of the UPR sensors relays information on the protein folding status from the ER lumen to the nucleus, thereby controlling gene expression. The PERK branch was described to control the expression of miR-708 (Behrman et al. 2011), miR-106b-25 (Gupta et al. 2012), miR-30c-2* (Byrd et al. 2012) and miR-211 (Chitnis et al. 2012). In the same way, ATF6 signaling down-regulates the expression of miR-455 (Belmont et al. 2012) and *IRE1 α* signaling increases that of miR-346 (Bartoszewski et al. 2011). Recently, miR-122, the most abundant miRNA in the liver, whose expression is repressed in HCC, was found to inhibit CDK4, which interacts and induces accumulation of PSMD10, a proteasome component and an enhancer of the UPR (Yang et al. 2011). Herein, we describe for the first time a miRNA acting as an upstream inhibitor of the UPR pathway by directly targeting *IRE1 α* expression. Intriguingly, this regulation did not depend on ER stress. As the same *IRE1 α* -dependent cleavage under unstressed conditions was also observed for *SCARA3* mRNA (this study) and *SPARC* mRNA (Dejeans et al. 2012) one might suggest potential roles for UPR signaling components in non-stressed conditions as also recently described for *IRE1* and *PERK* (Tam et al. 2012).

Fine-tuning of the UPR plays a fundamental role in cancer cell fate decisions by determining adaptation and survival to ER stress, and eliminating irreversibly damaged cells (Moenner et al. 2007; Tabas and Ron 2011; Woehlbier and Hetz 2011). In this context, IRE1 α has evolved a dual function to preserve ER homeostasis (Han et al. 2009). First, the IRE1 α /XBP1 axis is thought to favor tumor cell adaptation to stress by increasing the ability of these cells to synthesize and fold large amounts of transmembrane and secreted proteins. Second, prolonged activation of the RIDD pathway might decrease tumor growth in a cell-specific manner by degrading mRNAs encoding pro-oncogenic proteins, including PDGFR and SPARC (Hollien and Weissman 2006; Dejeans et al. 2012). In the present study, we identify *GPC3* mRNA as a novel RIDD substrate and demonstrate its cleavage by IRE1 α endoribonuclease at a consensus site located in *GPC3* mRNA 3'-UTR (Fig. 7 and 8). *GPC3* is known to promote HCC cell growth by stimulating the WNT/ β -catenin pathway (Capurro et al. 2005). Consequently our results suggest that miR-1291 could act as an oncomiR by attenuating IRE1 α expression and RIDD, thereby leading to *GPC3* overexpression in liver tumors. This hypothesis should however be considered carefully as in the mean time miR-1291-mediated attenuation of *IRE1\alpha* expression would also reduce *XBP1* mRNA splicing. The integrated signaling outcomes resulting from this initial event would therefore determine the oncogenic potential of miR-1291. Finally, although it is currently believed that IRE1 α activation plays an instrumental role in tumor progression (Auf et al. 2010; Dejeans et al. 2012), somatic driver mutations in the IRE1 α gene were identified in cancers (Greenman et al. 2007) and recently associated with a loss-of-signaling function of this molecule (Xue et al. 2011), thereby also associating IRE1 α inactivation with cell transformation. This might be consistent with the hypothesis of a pro-oncogenic miR-1291-mediated attenuation of IRE1 α signaling.

In conclusion, we report a novel mechanism of miRNA-mediated positive regulation of gene expression originating from the silencing of the endoribonuclease IRE1 α (Fig. 9). The physiological and pathophysiological consequences of such mechanism still remain to be fully investigated, especially in liver cancers in which *GPC3* overexpression plays a master regulatory role. However one can easily anticipate a significant contribution of *IRE1\alpha* down-regulation to cancer development through the overexpression of cancer-associated downstream gene targets.

Materials and Methods

Plasmids and cloning - The pL-eGFP-GPC3 3'-UTR lentiviral and pED-IRE1 α plasmids were as described previously (Nguyen et al. 2004; Maurel et al. 2013). The pEF-hGPC3 plasmid was kindly provided by S. Mizushima and S. Nagata (Osaka Bioscience Institute, Japan) (Mizushima and Nagata 1990). The pcDNA3.1- Δ CUACAG-hGPC3 was obtained as follows: a mutant *GPC3* gene devoid of the IRE1 α cleavage site was synthesized (Eurofins MWG Operon), digested by NotI and cloned into the pcDNA3.1 vector (Invitrogen, Carlsbad, CA, USA). The pL-wt-IRE1 α 5'-UTR-eGFP and pL-mut-IRE1 α -5'-UTR-eGFP plasmids were constructed as follows: IRE1 α 5'-UTR was amplified using 5'-CACGGATCCTGCCTAGTCAGTTCTGCGTC as forward primer and either 5'-CACGGATCCGGCGAGGACTCGGCCCT or 5'-CACGGATCCGGCGAGGACTCCGGCGTGGCTCCGGGGG as reverse primers, respectively. Each PCR product was digested by BamHI and sub-cloned into pL-eGFP plasmid (Maurel et al. 2013). Sequence was verified by DNA sequencing.

Cell culture

HuH7 cells were grown in DMEM (Invitrogen, Carlsbad, CA, USA) containing 10% Fetal Bovine Serum (FBS) and penicillin/streptomycin (1000 units/mL). Enhanced green Fluorescent protein (eGFP)-expressing HuH7 cells were established using lentiviral transduction (m.o.i. =3) as previously described (Laloo et al. 2009; Jalvy-Delvaile et al. 2012). Tunicamycin (Tun; 10 μ g/mL) was from Calbiochem (EMD Biosciences Inc., Darmstadt, Germany). Dithiothreitol (DTT; 2mM) and Actinomycin D (5 μ g/mL) were obtained from Sigma.

Small RNA transfection - Small inhibitory RNAs (siRNAs, Supplementary Table S1) were designed using the Greg Hannon's webtool (<http://hannonlab.cshl.edu/>). The negative control RNA, mature miRNA mimics and hairpin miRNA inhibitors were from Qiagen (Hilden, Germany). Unless otherwise stated, small RNAs were transfected into the target cells at 12 nM by reverse-transfection using Lipofectamine RNAi Max (Invitrogen, Carlsbad, CA, USA) following the manufacturer's instructions.

RNA isolation, Reverse Transcription and qPCR analyses - Total RNA was prepared using the TRI Reagent (Sigma, StLouis, MO, USA) following the manufacturer's instructions. Mature miRNA expression was quantified using the TaqMan microRNA Reverse Transcription Kit and TaqMan microRNA assays (Applied Biosystems, Carlsbad, CA, USA). Messenger RNA expression was quantified using the SYBR Green Supermix (Quanta Biosciences, Gaithersburg, MD, USA). Quantitative PCR reactions were performed using the Step One Plus Quantitative PCR System (Applied Biosystems, Carlsbad, CA, USA). For each data point, experiments were performed in triplicate. In all cases, each sample was normalized toward the expression of the 18S ribosomal RNA. Absolute quantification was performed using a standard curve-based approach. Standard curve was obtained using serial dilutions of plasmid or miRNA of known concentrations on a tenfold basis. The copy number was calculated as follows: $X \text{ g/mol} / \text{Avogadro's number} = X \text{ g/molecule}$. Standard curves were obtained by plotting the crossing threshold (Ct) against the log number of molecules. The equation drawn from the graph was used to calculate the precise number of target molecule tested in same reaction plate as standard as well as in sample. PCR products were resolved on 1% agarose TBE 0.5x electrophoresis gels or 4% for the *XBP1* splicing experiments. Primers used are as described in Supplementary Table S2. For ER-associated RNA enrichment, an immuno-isolation approach was undertaken as previously described (Nguyen et al. 2004). Briefly, HuH7 cells were homogenized using a teflon potter in the presence of RNAsin and homogenates were clarified by centrifugation at 1500g for 10 min. Clarified homogenates were incubated in the presence of anti calnexin antibodies for 2h and then magnetic beads were added for additional 20 min at 4°C. Beads were collected using a magnet and washed extensively. Purified ER membranes were then treated with Trizol, RNA extracted and reverse transcribed.

Antibodies and Western blot analyses - Antibody against GPC3 was from Biomosaics (Burlington, NC, USA). Anti IRE1 α and anti GAPDH were from Santa-Cruz Biotechnology (Santa Cruz, CA, USA). Protein extraction and Western blotting were performed as previously described (Jalvy-Delville et al. 2012). Signals were normalized to the amount of the housekeeping protein GAPDH.

FunREG analyses - FunREG analyses were performed three days after cell transfection as previously described (Laloo *et al.* 2009; Maurel *et al.* 2013). Cells were washed with PBS, detached with trypsin/EDTA, collected and analyzed by FACS using the BD LSRFortessa cell analyzer and the BD FACSDiva software (BD Biosciences, San Jose, CA, USA). In parallel, genomic DNA and total RNA were extracted by TRI Reagent (see above) from each cell population. Quantitative RT-PCR was performed as described above. The transgene copy number (TCN) was measured by quantitative PCR using genomic DNA as described previously (Laloo *et al.* 2009; Jalvy-Delvaile *et al.* 2012).

Bioinformatic analyses - *In silico* analyses were performed using miRWalk (Dweep *et al.* 2011). This program identifies the longest consecutive complementarity between miRNA and gene sequences, produces information about miRNA:target interactions on the complete gene sequence (promoter, 5'-UTR, coding sequence and 3'-UTR) of all known genes and compares the candidate miRNA binding sites with those established by 8 miRNA-target prediction programs (i.e. DIANA-microT, miRanda, miRDB, PicTar, PITA, RNA22, RNAhybrid and TargetScan/TargetScanS). Finally miRWalk incorporates all the predicted miRNA binding sites produced by the miRWalk algorithm and the 8 other programs into a relational database. The secondary structure of the *GPC3* mRNA:miR-1291 interaction was predicted using M-FOLD (Zuker *et al.* 1999). Functional classification was achieved by g:profiler (Reimand *et al.* 2007). Generated data were also manually sorted and integrated to generate quantitative and qualitative information on the Gene Ontology (Cellular Compartment and Biological Process components). Moreover an additional piece of information concerning candidate miR-1291 targets was retrieved from databases (GeneCard, NCBI, miRBase, miRDB, HNGC) and from the literature to constitute a binary (No = 0; Yes = 1) annotation file. A scoring system was established based on the methodology previously described for integration of heterogenous data for gene function prediction (Troyanskaya *et al.* 2003). Scores were then clustered. All these data were then clustered and represented using the CLUSTER and TREEVIEW programs (Hoon *et al.* 2004; Saldanha 2004). All the clusters were built using Euclidian distances. Trees were generated using average linkage.

RNA cleavage assay - Ten μg of total RNA extracted from HuH7 were incubated at 37°C with the cytoplasmic domain of human IRE1 α (5 μg) fused to GST (GST-IRE1 α^{cyto}) for 4h in a buffer containing 25 mM Tris-HCl (pH 7.5), 0.5 mM MgCl₂ and 1 mM ATP, as previously described (Bouchecareilh *et al.* 2010; Bouchecareilh *et al.* 2011). Heat-denatured GST-IRE1 α^{cyto} was used as control. RNA fragments were detected by RT-PCR using specific primers (Supplementary Table S2). The pcDNA3.1- Δ CUACAG-hGPC3 and pEF-hGPC3 plasmids were used as template for *in vitro* RNA transcription using the T7 polymerase (Promega, Madison, WI, USA). *In vitro* transcribed RNA was incubated at 37°C with 5 μg of GST-IRE1 α^{cyto} and 1 mM ATP for 4h. Reaction products were then denatured 10 minutes at 65°C in RNA sample Buffer (56% formamide, 37% formaldehyde, 7% MOPS). Fragments resulting from the enzymatic reaction were resolved on 1% formaldehyde agarose gels and visualized by UV trans-illumination.

Statistical analyses - Statistical analyses were performed using GraphPad Prism 5.0 software (La Jolla, CA, USA). Data are presented as the mean of the indicated number of independent experiments \pm standard deviation (SD). When experiment contained three groups of values or more, regular one-way analysis of variance (ANOVA) was used for the comparison of multiple means. Means were considered significantly different when $P < 0.05$. The ANOVA test was followed by a Bonferroni's multiple-comparison post-test and selected pairs of data were compared. Significant variations are indicated with asterisks.

Acknowledgements

This work was funded in part by grants from L'Institut National du Cancer (INCa; project « INCa_5828 ») and La Ligue Nationale contre le Cancer (LNCC) to CG and INSERM, INCa (INCa_5869; INCa_2012_117), LNCC to EC. EC was supported by an Interface contract INSERM-CHU de Bordeaux. MM was a recipient from a PhD scholarship from the French Research Ministry. ND was funded by post-doctoral fellowships from LNCC and Fondation de France.

Accepted version

References

- Auf G, Jabouille A, Guerit S, Pineau R, Delugin M, Bouchecareilh M, Magnin N, Favereaux A, Maitre M, Gaiser T et al. 2010. Inositol-requiring enzyme 1alpha is a key regulator of angiogenesis and invasion in malignant glioma. *Proc Natl Acad Sci U S A* **107**(35): 15553-15558.
- Avraham R, Yarden Y. 2012. Regulation of signalling by microRNAs. *Biochem Soc Trans* **40**(1): 26-30.
- Bartel DP. 2009. MicroRNAs: target recognition and regulatory functions. *Cell* **136**(2): 215-233.
- Bartoszewski R, Brewer JW, Rab A, Crossman DK, Bartoszezowska S, Kapoor N, Fuller C, Collawn JF, Bebok Z. 2011. The unfolded protein response (UPR)-activated transcription factor X-box-binding protein 1 (XBP1) induces microRNA-346 expression that targets the human antigen peptide transporter 1 (TAP1) mRNA and governs immune regulatory genes. *J Biol Chem* **286**(48): 41862-41870.
- Behm-Ansmant I, Rehwinkel J, Doerks T, Stark A, Bork P, Izaurralde E. 2006. mRNA degradation by miRNAs and GW182 requires both CCR4:NOT deadenylase and DCP1:DCP2 decapping complexes. *Genes Dev* **20**(14): 1885-1898.
- Behrman S, Acosta-Alvear D, Walter P. 2011. A CHOP-regulated microRNA controls rhodopsin expression. *J Cell Biol* **192**(6): 919-927.
- Belmont PJ, Chen WJ, Thuerauf DJ, Glembotski CC. 2012. Regulation of microRNA expression in the heart by the ATF6 branch of the ER stress response. *J Mol Cell Cardiol* **52**(5): 1176-1182.
- Bouchecareilh M, Caruso ME, Roby P, Parent S, Rouleau N, Taouji S, Pluquet O, Bosse R, Moenner M, Chevet E. 2010. AlphaScreen-based characterization of the bifunctional kinase/RNase IRE1alpha: a novel and atypical drug target. *J Biomol Screen* **15**(4): 406-417.
- Bouchecareilh M, Higa A, Fribourg S, Moenner M, Chevet E. 2011. Peptides derived from the bifunctional kinase/RNase enzyme IRE1alpha modulate IRE1alpha activity and protect cells from endoplasmic reticulum stress. *FASEB J* **25**(9): 3115-3129.
- Brameier M, Herwig A, Reinhardt R, Walter L, Gruber J. 2011. Human box C/D snoRNAs with miRNA like functions: expanding the range of regulatory RNAs. *Nucleic Acids Res* **39**(2): 675-686.
- Bruno IG, Karam R, Huang L, Bhardwaj A, Lou CH, Shum EY, Song HW, Corbett MA, Gifford WD, Gecz J et al. 2011. Identification of a microRNA that activates gene expression by repressing nonsense-mediated RNA decay. *Mol Cell* **42**(4): 500-510.
- Byrd AE, Aragon IV, Brewer JW. 2012. MicroRNA-30c-2* limits expression of proadaptive factor XBP1 in the unfolded protein response. *J Cell Biol* **196**(6): 689-698.
- Calfon M, Zeng H, Urano F, Till JH, Hubbard SR, Harding HP, Clark SG, Ron D. 2002. IRE1 couples endoplasmic reticulum load to secretory capacity by processing the XBP-1 mRNA. *Nature* **415**(6867): 92-96.
- Capurro MI, Xiang YY, Lobe C, Filmus J. 2005. Glypican-3 promotes the growth of hepatocellular carcinoma by stimulating canonical Wnt signaling. *Cancer Res* **65**(14): 6245-6254.
- Chitnis NS, Pytel D, Bobrovnikova-Marjon E, Pant D, Zheng H, Maas NL, Frederick B, Kushner JA, Chodosh LA, Koumenis C et al. 2012. miR-211 is a prosurvival

- microRNA that regulates chop expression in a PERK-dependent manner. *Mol Cell* **48**(3): 353-364.
- Dejeans N, Pluquet O, Lhomond S, Grise F, Bouche-careilh M, Juin A, Meynard-Cadars M, Bidaud-Meynard A, Gentil C, Moreau V et al. 2012. Autocrine control of glioma cells adhesion/migration through Inositol Requiring enzyme 1alpha (IRE1alpha)-mediated cleavage of Secreted Protein Acidic Rich in Cysteine (SPARC) mRNA. *J Cell Sci*.
- Dweep H, Sticht C, Pandey P, Gretz N. 2011. miRWalk--database: prediction of possible miRNA binding sites by "walking" the genes of three genomes. *J Biomed Inform* **44**(5): 839-847.
- Fabian MR, Sonenberg N, Filipowicz W. 2010. Regulation of mRNA translation and stability by microRNAs. *Annu Rev Biochem* **79**: 351-379.
- Filmus J, Capurro M, Rast J. 2008. Glypicans. *Genome Biol* **9**(5): 224.
- Fransson LA. 2003. Glypicans. *Int J Biochem Cell Biol* **35**(2): 125-129.
- Gaddam D, Stevens N, Hollien J. 2013. Comparison of mRNA localization and regulation during endoplasmic reticulum stress in *Drosophila* cells. *Mol Biol Cell* **24**(1): 14-20.
- Greenman C, Stephens P, Smith R, Dalgliesh GL, Hunter C, Bignell G, Davies H, Teague J, Butler A, Stevens C et al. 2007. Patterns of somatic mutation in human cancer genomes. *Nature* **446**(7132): 153-158.
- Griffiths-Jones S, Saini HK, van Dongen S, Enright AJ. 2008. miRBase: tools for microRNA genomics. *Nucleic Acids Res* **36**(Database issue): D154-158.
- Gupta S, Read DE, Deepti A, Cawley K, Gupta A, Oommen D, Verfaillie T, Matus S, Smith MA, Mott JL et al. 2012. Perk-dependent repression of miR-106b-25 cluster is required for ER stress-induced apoptosis. *Cell Death Dis* **3**: e333.
- Han D, Lerner AG, Vande Walle L, Upton JP, Xu W, Hagen A, Backes BJ, Oakes SA, Papa FR. 2009. IRE1alpha kinase activation modes control alternate endoribonuclease outputs to determine divergent cell fates. *Cell* **138**(3): 562-575.
- Hidaka H, Seki N, Yoshino H, Yamasaki T, Yamada Y, Nohata N, Fuse M, Nakagawa M, Enokida H. 2012. Tumor suppressive microRNA-1285 regulates novel molecular targets: aberrant expression and functional significance in renal cell carcinoma. *Oncotarget* **3**(1): 44-57.
- Hollien J, Lin JH, Li H, Stevens N, Walter P, Weissman JS. 2009. Regulated Ire1-dependent decay of messenger RNAs in mammalian cells. *J Cell Biol* **186**(3): 323-331.
- Hollien J, Weissman JS. 2006. Decay of endoplasmic reticulum-localized mRNAs during the unfolded protein response. *Science* **313**(5783): 104-107.
- Hoon DS, Spugnardi M, Kuo C, Huang SK, Morton DL, Taback B. 2004. Profiling epigenetic inactivation of tumor suppressor genes in tumors and plasma from cutaneous melanoma patients. *Oncogene* **23**(22): 4014-4022.
- Huang V, Place RF, Portnoy V, Wang J, Qi Z, Jia Z, Yu A, Shuman M, Yu J, Li LC. 2012. Upregulation of Cyclin B1 by miRNA and its implications in cancer. *Nucleic Acids Res* **40**(4): 1695-1707.
- Huntzinger E, Izaurralde E. 2011. Gene silencing by microRNAs: contributions of translational repression and mRNA decay. *Nat Rev Genet* **12**(2): 99-110.
- Iqbal J, Dai K, Seimon T, Jungreis R, Oyadomari M, Kuriakose G, Ron D, Tabas I, Hussain MM. 2008. IRE1beta inhibits chylomicron production by selectively degrading MTP mRNA. *Cell Metab* **7**(5): 445-455.

- Jakubovic BD, Jothy S. 2007. Glypican-3: from the mutations of Simpson-Golabi-Behmel genetic syndrome to a tumor marker for hepatocellular carcinoma. *Exp Mol Pathol* **82**(2): 184-189.
- Jalvy-Delvaile S, Maurel M, Majo V, Pierre N, Chabas S, Combe C, Rosenbaum J, Saggiocco F, Grosset CF. 2012. Molecular basis of differential target regulation by miR-96 and miR-182: the Glypican-3 as a model. *Nucleic Acids Res* **40**(3): 1356-1365.
- Kozomara A, Griffiths-Jones S. 2011. miRBase: integrating microRNA annotation and deep-sequencing data. *Nucleic Acids Res* **39**(Database issue): D152-157.
- Laloo B, Maurel M, Jalvy-Delvaile S, Saggiocco F, Grosset CF. 2010. Analysis of post-transcriptional regulation using the FunREG method. *Biochem Soc Trans* **38**(6): 1608-1614.
- Laloo B, Simon D, Veillat V, Lauzel D, Guyonnet-Duperat V, Moreau-Gaudry F, Saggiocco F, Grosset C. 2009. Analysis of post-transcriptional regulations by a functional, integrated, and quantitative method. *Mol Cell Proteomics* **8**(8): 1777-1788.
- Lerner RS, Seiser RM, Zheng T, Lager PJ, Reedy MC, Keene JD, Nicchitta CV. 2003. Partitioning and translation of mRNAs encoding soluble proteins on membrane-bound ribosomes. *RNA* **9**(9): 1123-1137.
- Ma F, Liu X, Li D, Wang P, Li N, Lu L, Cao X. 2010. MicroRNA-466l upregulates IL-10 expression in TLR-triggered macrophages by antagonizing RNA-binding protein tristetraprolin-mediated IL-10 mRNA degradation. *J Immunol* **184**(11): 6053-6059.
- Maurel M, Jalvy S, Ladeiro Y, Combe C, Vachet L, Saggiocco F, Bioulac-Sage P, Pitard V, Jacquemin-Sablon H, Zucman-Rossi J et al. 2013. A functional screening identifies five micrnas controlling glypican-3: role of mir-1271 down-regulation in hepatocellular carcinoma. *Hepatology* **57**(1): 195-204.
- Meder B, Keller A, Vogel B, Haas J, Sedaghat-Hamedani F, Kayvanpour E, Just S, Borries A, Rudloff J, Leidinger P et al. 2011. MicroRNA signatures in total peripheral blood as novel biomarkers for acute myocardial infarction. *Basic Res Cardiol* **106**(1): 13-23.
- Mizushima S, Nagata S. 1990. pEF-BOS, a powerful mammalian expression vector. *Nucleic Acids Res* **18**(17): 5322.
- Moenner M, Pluquet O, Bouche-careilh M, Chevet E. 2007. Integrated endoplasmic reticulum stress responses in cancer. *Cancer Res* **67**(22): 10631-10634.
- Nguyen DT, Kebache S, Fazel A, Wong HN, Jenna S, Emadali A, Lee EH, Bergeron JJ, Kaufman RJ, Larose L et al. 2004. Nck-dependent activation of extracellular signal-regulated kinase-1 and regulation of cell survival during endoplasmic reticulum stress. *Mol Biol Cell* **15**(9): 4248-4260.
- Oikawa D, Tokuda M, Hosoda A, Iwawaki T. 2010. Identification of a consensus element recognized and cleaved by IRE1 alpha. *Nucleic Acids Res* **38**(18): 6265-6273.
- Orom UA, Nielsen FC, Lund AH. 2008. MicroRNA-10a binds the 5'UTR of ribosomal protein mRNAs and enhances their translation. *Mol Cell* **30**(4): 460-471.
- Pillai RS, Bhattacharyya SN, Filipowicz W. 2007. Repression of protein synthesis by miRNAs: how many mechanisms? *Trends Cell Biol* **17**(3): 118-126.
- Pyhtila B, Zheng T, Lager PJ, Keene JD, Reedy MC, Nicchitta CV. 2008. Signal sequence- and translation-independent mRNA localization to the endoplasmic reticulum. *RNA* **14**(3): 445-453.

- Rehmsmeier M, Steffen P, Hochsmann M, Giegerich R. 2004. Fast and effective prediction of microRNA/target duplexes. *RNA* **10**(10): 1507-1517.
- Reimand J, Kull M, Peterson H, Hansen J, Vilo J. 2007. g:Profiler--a web-based toolset for functional profiling of gene lists from large-scale experiments. *Nucleic Acids Res* **35**(Web Server issue): W193-200.
- Saldanha AJ. 2004. Java Treeview--extensible visualization of microarray data. *Bioinformatics* **20**(17): 3246-3248.
- Schroder M, Kaufman RJ. 2005. The mammalian unfolded protein response. *Annu Rev Biochem* **74**: 739-789.
- Scott MS, Avolio F, Ono M, Lamond AI, Barton GJ. 2009. Human miRNA precursors with box H/ACA snoRNA features. *PLoS Comput Biol* **5**(9): e1000507.
- Shirakawa H, Suzuki H, Shimomura M, Kojima M, Gotohda N, Takahashi S, Nakagohri T, Konishi M, Kobayashi N, Kinoshita T et al. 2009. Glypican-3 expression is correlated with poor prognosis in hepatocellular carcinoma. *Cancer Sci* **100**(8): 1403-1407.
- Tabas I, Ron D. 2011. Integrating the mechanisms of apoptosis induced by endoplasmic reticulum stress. *Nat Cell Biol* **13**(3): 184-190.
- Tam AB, Mercado EL, Hoffmann A, Niwa M. 2012. ER stress activates NF-kappaB by integrating functions of basal IKK activity, IRE1 and PERK. *PLoS One* **7**(10): e45078.
- Troyanskaya OG, Dolinski K, Owen AB, Altman RB, Botstein D. 2003. A Bayesian framework for combining heterogeneous data sources for gene function prediction (in *Saccharomyces cerevisiae*). *Proc Natl Acad Sci U S A* **100**(14): 8348-8353.
- Vasudevan S. 2012. Posttranscriptional upregulation by microRNAs. *Wiley Interdiscip Rev RNA* **3**(3): 311-330.
- Vasudevan S, Tong Y, Steitz JA. 2007. Switching from repression to activation: microRNAs can up-regulate translation. *Science* **318**(5858): 1931-1934.
- Walter P, Ron D. 2011. The unfolded protein response: from stress pathway to homeostatic regulation. *Science* **334**(6059): 1081-1086.
- Woehlbier U, Hetz C. 2011. Modulating stress responses by the UPRosome: a matter of life and death. *Trends Biochem Sci* **36**(6): 329-337.
- Xue Z, He Y, Ye K, Gu Z, Mao Y, Qi L. 2011. A conserved structural determinant located at the interdomain region of mammalian inositol-requiring enzyme 1alpha. *J Biol Chem* **286**(35): 30859-30866.
- Yang F, Zhang L, Wang F, Wang Y, Huo XS, Yin YX, Wang YQ, Sun SH. 2011. Modulation of the unfolded protein response is the core of microRNA-122-involved sensitivity to chemotherapy in hepatocellular carcinoma. *Neoplasia* **13**(7): 590-600.
- Zuker M, Mathews DH, Turner DH. 1999. Algorithms and Thermodynamics for RNA Secondary Structure Prediction: A Practical Guide. *RNA Biochemistry and Biotechnology*.

Figure Legends

Figure 1: MiR-1291 specifically enhances GPC3 mRNA stability through its 3'-UTR. Top panel: schematic representation of the eGFP-GPC3 3'-UTR transgene used in this study. Bottom panel: eGFP-GPC3 3'-UTR-expressing HuH7 cells were transfected with a control RNA or miR-1291. Three days later, the transgene copy number (TCN) and the expression of eGFP protein (P) and mRNA (M) were measured. Finally the FunREG ratios were calculated as described in the Materials and Methods section. P/TCN: global post-transcriptional regulation, M/TCN: mRNA stability and P/M: translation efficiency (ANOVA: $P < 0.0001$; $n = 5$). $**p < 0.01$.

Figure 2: MiR-1291 targets an intermediate factor that regulates GPC3 mRNA expression. (A) Selection of miR-1291-predicted targets involved in mRNA destabilization. Using miRWalk, 2782 gene candidates were predicted as miR-1291 targets (p -value < 0.01). Among them, 83 are described as post-transcriptional regulators. A hierarchical clustering was performed for seven candidate genes that were identified as relevant of a membranous compartment, namely *ERN1*, *TIRAP*, *BICD1*, *CHERP*, *TLR7*, *SLC11A1* and *TRMU*. Scale bar is indicated. (B) Identification of three sites homologous to the 5'-CUGCAG-3' IRE1 α consensus cleavage site in *GPC3* mRNA (red). (C) IRE1 α inhibits eGFP-GPC3 3'UTR mRNA stability. EGFP-GPC3 3'-UTR-expressing HuH7 cells were transfected with an empty vector or *IRE1 α* vector. Three days later, the expression of eGFP mRNA was measured. (ANOVA: $P < 0.0001$; $n = 3$). $*p < 0.1$. (D) Whereas miR-1291 increases *GPC3* expression, it decreases that of *IRE1 α* . HuH7 cells were transfected with a control miRNA and miR-1291. The relative expression of *IRE1 α* and *GPC3* mRNA was measured using RT-qPCR (ANOVA: $P < 0.0001$; $n = 10$). $***p < 0.001$. (E) HuH7 cells were transfected with increasing concentrations of anti-miR-1291 (AM1291). The relative expression of *IRE1 α* and *GPC3* mRNA was measured using RT-qPCR (ANOVA: $P < 0.0001$; $n = 3$). $***p < 0.001$.

Figure 3: MiR-1291 targets and destabilizes IRE1 α mRNA through its 5'-UTR. (A) *IRE1 α* 5'UTR contains a potential miR-1291 binding site. Schematic representation of miR-1291/*IRE1 α* 5'UTR interaction using RNAhybrid. (B) Top panel: schematic representation of *IRE1 α* 5'-UTR-eGFP transgene. Bottom panel: Schematic

representation of miR-1291 pairing with *IRE1α* 5'-UTR in its wild type or mutated form. **(C)** HuH7 cells expressing the indicated transgenes were transfected with the indicated small RNAs. Three days later, eGFP protein expression was measured (ANOVA: $P < 0.0001$; $n = 3$). $***p < 0.001$. **(D)** HuH7 cells expressing the wt-*IRE1α* 5'-UTR-eGFP transgene were transfected with a control RNA or miR-1291. After 3 days, FunREG ratios were calculated as described in Figure 1 (ANOVA: $P < 0.0001$; $n = 4$). $***p < 0.001$. **(E)** Overexpression of *IRE1α* lacking its mRNA 5'-UTR counteracts miR-1291-mediated increase in *GPC3* mRNA. HuH7 cells were transfected with the indicated plasmid and small RNA. Then *GPC3* mRNA expression was measured using RT-qPCR (ANOVA: $P < 0.0001$; $n = 5$). $*p < 0.05$; $**p < 0.01$; $***p < 0.001$.

Figure 4: *IRE1α*-silencing increases *GPC3* mRNA independently of ER stress.

(A) *IRE1α* mediates *XBP1* mRNA splicing upon ER stress. ER stress-induced splicing of *XBP1* mRNA yields a transcript with a 26-nucleotide deletion in comparison to the unspliced transcript. HuH7 cells transfected with the indicated siRNAs were exposed to dithiothreitol (DTT) for 6h or to tunicamycin (Tun) for 24h. Then *XBP1* mRNA splicing was monitored by RT-PCR. **(B-C)** *IRE1α*-silencing increases *GPC3* expression. HuH7 cells were transfected with the indicated small RNA and then treated or not with DTT or Tun. Three days later, mRNA and protein expression (ANOVA: $P < 0.0001$; $n = 8$) was measured by qPCR **(B)** and Western blotting **(C)**. *GPC3* and non-glycosylated *GPC3* (ng*GPC3*) proteins were as shown. $***p < 0.001$.

Figure 5: MiR-1291 specifically alters *IRE1α* signaling independently of ER stress.

(A-B) Overexpression of miR-1291 did not affect ATF6 and PERK signaling upon Tun treatment. HuH7 cells transfected with the indicated small RNA were exposed to Tun (24h). **(A)** The relative expression of *HERPUD* and *GRP94* mRNAs was measured using RT-qPCR (ANOVA: $P < 0.0001$; $n = 5$). $*p < 0.05$. **(B)** *CHOP* mRNA expression was measured (ANOVA: $P < 0.0001$; $n = 5$). $***p < 0.001$. **(C)** MiR-1291 selectively affects *IRE1α* signaling. Top panel: HuH7 cells transfected with the indicated small RNA were exposed to DTT (6h). Then *XBP1* mRNA splicing was monitored. The results are representative of 5 independent experiments. Bottom panel: HuH7 cells transfected with the indicated small RNA were exposed to Tun

(24h). Then the relative expression of *PDGFR*, *COL1* and *SCARA3* mRNAs was measured (ANOVA: $P < 0.0001$; $n = 5$). ** $p < 0.001$; *** $p < 0.001$.

Figure 6: IRE1 α -silencing leads to *GPC3* mRNA stabilization. (A) HuH7 cells were transfected with the indicated small RNA. Three days later, *GPC3* and *ALB* mRNA were measured at different times following transcription inhibition using actinomycin D (ANOVA: $P < 0.0001$; $n = 3$). * $p < 0.05$; ** $p < 0.01$. (B) HuH7 cells were exposed or not to Tun (24h). Then, *GPC3* expression was measured following transcription inhibition using actinomycin D or not (ANOVA: $P < 0.0001$; $n = 5$).

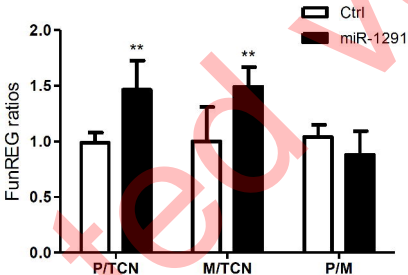
Figure 7: IRE1 α cleaves *GPC3* mRNA *in vitro* at a canonical site located in its 3'-UTR. (A) Three potential IRE1 α -mediated cleavage sites were identified in *GPC3* mRNA. Top: Sequence alignment of IRE1 α cleavage sites in *XBP1* and *GPC3* mRNAs. Bottom: Two-dimensional M-Fold RNA modeling of potential IRE1 α cleavage sites in *GPC3* mRNA. (B) IRE1 α cleaves *GPC3* mRNA within its 3'-UTR *in vitro*. Total RNA extracted from HuH7 cells was incubated with heat-inactivated or not GST-IRE1 α^{cyto} . IRE1 α -mediated cleavage of *GPC3* mRNA was monitored by PCR at the indicated site. (C-D) IRE1 α directly targets the 2039/40 cleavage site in *GPC3* 3'-UTR. (C) Expected *GPC3* mRNA products following IRE1 α -mediated cleavage at the 2039/40 site. (D) *In vitro*-transcribed wild type and IRE1 α -site deleted *GPC3* RNAs were incubated or not with heat-inactivated or not GST-IRE1 α^{cyto} in presence or absence of RNase H. Resulting reaction products were resolved on denaturing agarose gels.

Figure 8: IRE1 α cleaves *GPC3* mRNA in cultured cells. (A) Schematic representation of the expected *GPC3* mRNA products following IRE1 α -mediated cleavage and their subsequent regulation by the exonucleases XRN1 and XRN2, or the RNA helicase *SKI2*. (B) HuH7 cells were transfected with the indicated small RNAs. Three days later, the presence of the *GPC3* mRNA Fragment 1 and 2 was monitored using RT-qPCR (ANOVA: $P < 0.0001$; $n = 6$). * $p < 0.05$; ** $p < 0.01$; *** $p < 0.001$. (C-D) HuH7 cells were transfected with the indicated small RNAs. Three days later, *GPC3* fragment 1 (C) and the *GPC3* amplicon framing the IRE1 α cleavage site (D) were monitored using RT-qPCR (ANOVA: $P < 0.0001$; $n = 3$). * $p < 0.05$; ** $p < 0.01$.

Figure 9: MiR-1291 up-regulates *GPC3* through inhibition of *IRE1 α* expression.

Schematic representation of miR-1291-mediated *GPC3* up-regulation through inhibition of *IRE1 α* expression. The grey frame indicates the original observation that miR-1291 upregulates *GPC3* mRNA expression through its 3'-UTR (Maurel et al. 2013). The green dashed arrow indicates a positive and indirect regulation of *GPC3* mRNA expression. Red signs indicate negative and direct regulations.

Accepted version

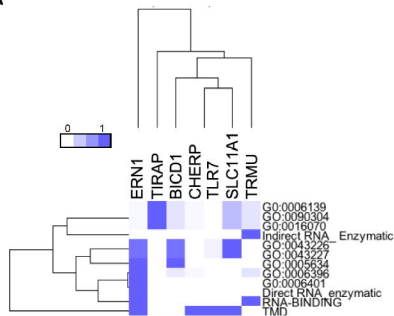


P/TCN : Global post-transcriptional regulation

M/TCN : mRNA stability

P/M : Translation efficiency

A

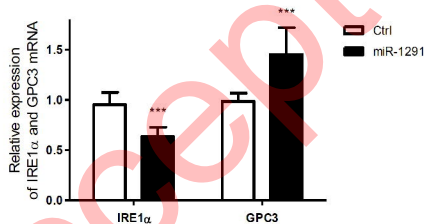


B

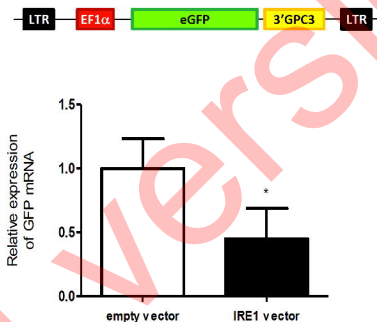
GPC3 (331/32) 5' CAGAGACU GCAGCCCG 3' ORF
 GPC3 (1494/95) 5' CUACAUCU GCAGCCAU 3' ORF
 GPC3 (2039/40) 5' GCUGCCCU ACAGACC 3' 3' UTR

Consensus 5' CU GCAG 3'

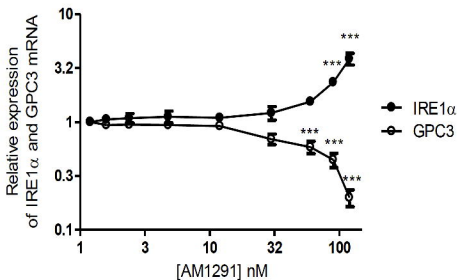
D



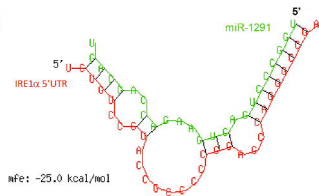
C



E



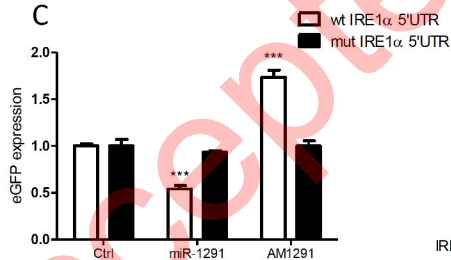
A



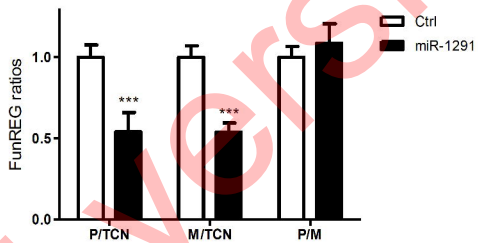
B



C



D

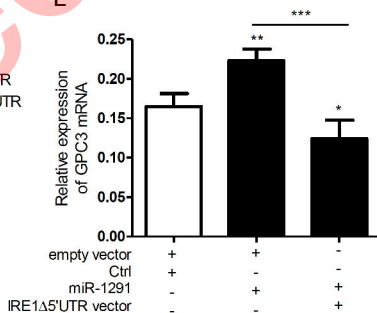


P/TCN : Global post-transcriptional regulation

M/TCN : mRNA stability

P/M : Translation efficiency

E



empty vector +

+

empty vector -

-

miR-1291 +

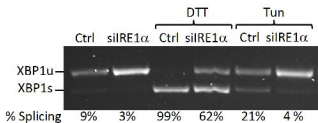
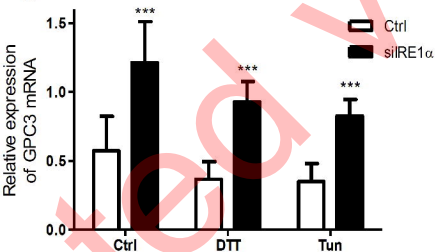
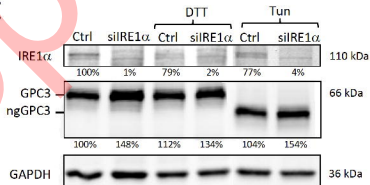
+

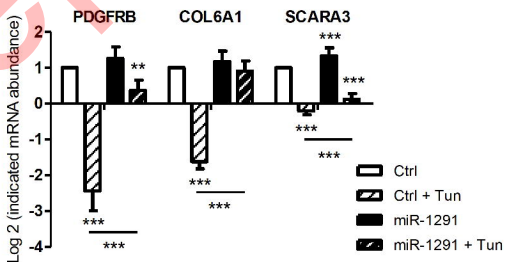
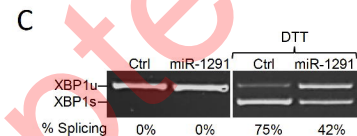
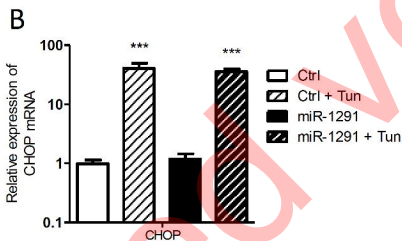
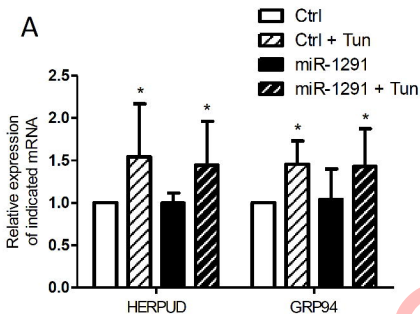
miR-1291 -

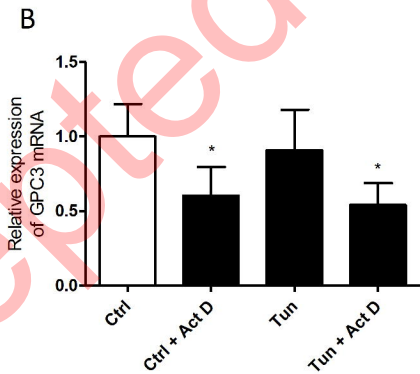
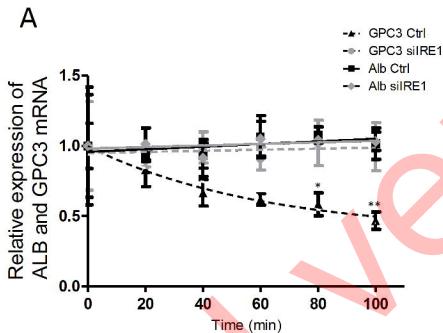
-

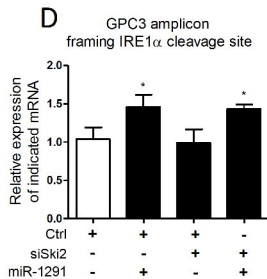
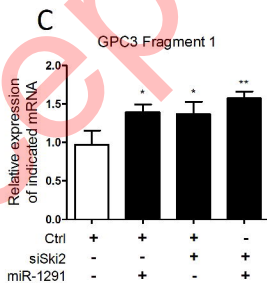
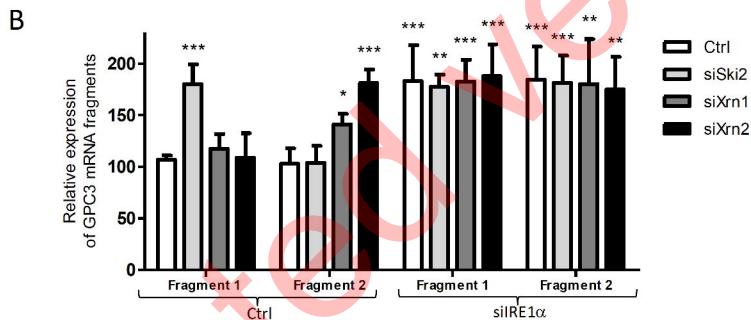
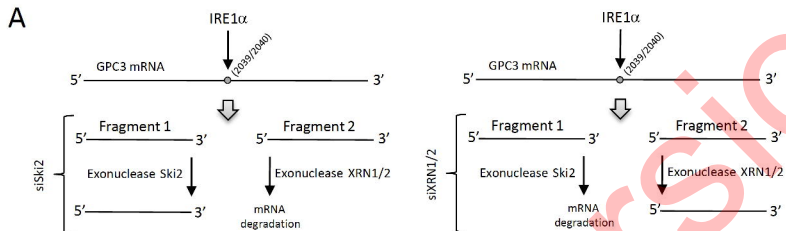
IRE1Δ5'UTR vector -

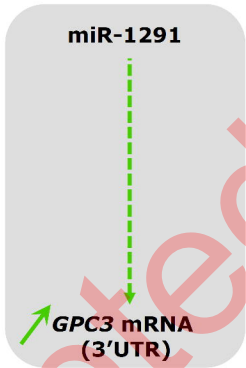
+

A**B****C**







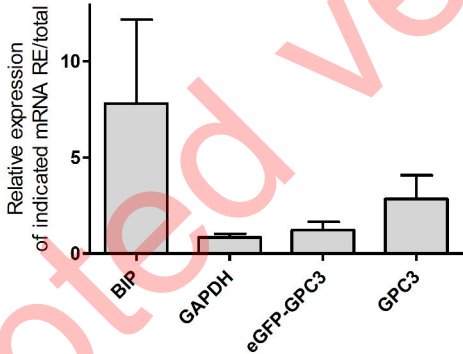


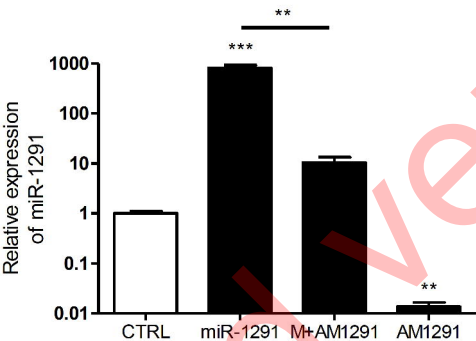
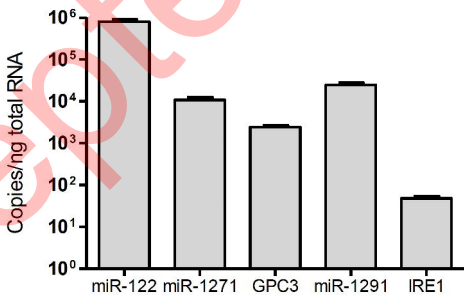
***IRE1 α* mRNA (5'UTR)**

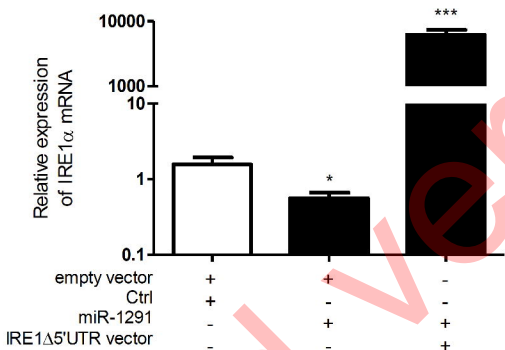
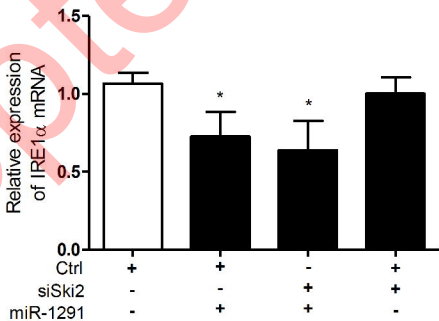


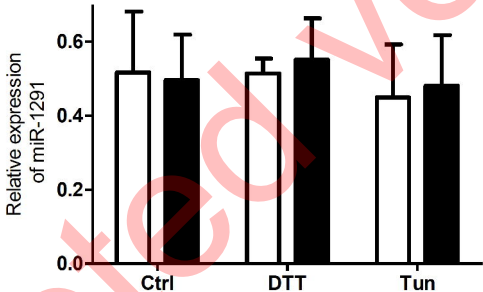
RIDD

IRE1 α



A**B**

A**B**



miRBase Accession:

RNA hybrid Predictions:

M-Fold Predictions:

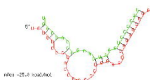
miR-1291 orthologues

miR-1291/IRE1 α 5'UTRConsensus IRE1 α cleavage site within GPC3 3'UTR***Homo sapiens***

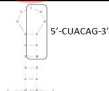
hsa-miR-1291

UGGCCCUGACUGAAGACCAGCAG***Pan troglodytes***

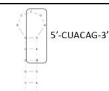
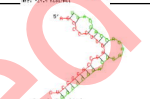
ptr-miR-1291

UGGCCCUGACUGAAGACCAGCAGU***Gorilla gorilla***

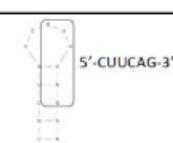
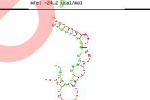
ggo-miR-1291

GUGGCCCUGACUGAAGACCAGCA***Pongo pygmaeus***

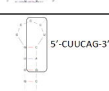
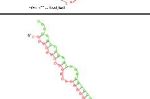
ppy-miR-1291

UGGCCCUGACUGAAGACCAGCAGU***Equus caballus***

eca-miR-1291a

UGGCCCUGACUGAAGACCAGCAGU***Equus caballus***

eca-miR-1291b

AGGCCCUGAAUCAAGACCAGCAGU***Bos taurus***

bta-miR-1291

UGGCCCUGACUGAAGACCUGCAGU

NP

